Hindawi
Wireless Communications and Mobile Computing
Volume 2022, Article ID 6838376, 11 pages
https://doi.org/10.1155/2022/6838376

Research Article

A Service-Aware Latency-Relaxed uRLLC Multiplexing Strategy within eMBB Traffic for Hyperloop Communications

Jiachi Zhang,[1,2] **Liu Liu**,[2] **Jiuhong Ruan**,[1] **Lu Li**,[1] **Kai Wang**,[2] **and Rongchen Sun**[3]

[1]*School of Rail Transportation, Shandong Jiaotong University, China 250357*
[2]*School of Electronic and Information Engineering, Beijing Jiaotong University, China 100044*
[3]*School of Information and Communication Engineering, Harbin Engineering University, Harbin, China 150001*

Correspondence should be addressed to Liu Liu; liuliu@bjtu.edu.cn

Received 26 January 2022; Revised 10 May 2022; Accepted 22 June 2022; Published 28 July 2022

Academic Editor: Pan Tang

The train-to-ground communications for Hyperloop encounter numerous challenges compared to the previous systems as a result of ultrahigh velocity, metal confined tube, severe penetration attenuation, frequent handover, etc. Ultrareliable low latency communication (uRLLC) services are extremely pivotal to the operation of Hyperloops since they are responsible for the transmission of safety-related messages like train control system (TCS) information. Furthermore, the sporadic generated uRLLC traffic is strictly latency-sensitive and requires stringent transmission reliability, which is usually realized by multiplexing with the enhanced mobile broadband (eMBB) traffic when coexisting with heterogeneous traffic. Different from current multiplexing schemes which handle all uRLLC traffic indiscriminately, we focus on the detailed demands of different uRLLC services for Hyperloops, including the end-to-end transmission latency and bit error rate (BER). Then, we classify the safety-related uRLLC traffic into 5 levels according to the metrics and relax the multiplexing latency properly. On this basis, an optimization problem incorporating minimizing uRLLC power and maximizing the eMBB throughput is formulated. Then, a particle swarm optimization (PSO) algorithm is proposed to cope with this nondeterministic polynomial- (NP-) hard problem. Simulation results imply that our proposed service-aware latency-relaxed concept enables a flexible multiplexing of the uRLLC traffic, and the proposed PSO algorithm can obtain the suboptimal solutions with the constraints of BER and time-frequency range, which can cater to the demands of uRLLC and improve the passengers' in-journey communication quality of services to some degree.

1. Introduction

The worldwide proliferation of high-speed railways (HSRs) yields great social-economic prosperity, regional development balance, user satisfaction, etc. [1]. For example, the top speed of Japanese Shinkanshen has risen from 210 km/h to 320 km/h, and it achieves a ridership of 1 million passengers per day. HSRs in Italy can reach a speed up to 400 km/h, which connect the main cities tightly. China has built over 40,000 kilometers of HSR lines by 2021 and expects to promote international development via the belt-and-road policy [2]. Despite the fastest high-speed train with a velocity of over 400 km/h, passengers are expecting to experience a more comfortable in-journey with less travel time. However, the acceleration of HSR is severely subject to the wheel-track mechanical friction, aerodynamics friction, and noise especially regarding the velocity over 500 km/h according to [3]. Furthermore, it is reported that the proportion of aerodynamic resistance in traction force will reach over 80% as the train speed exceeds 400 km/h, resulting in a huge waste of energy. Besides, the aerodynamic noise caused by high speed also rises sharply with the increase of speed, which is unbearable for onboard passengers.

Hyperloop, reported to proceed at a speed over 1000 km/h, is envisioned as the next-generation means of transportation and attracts numerous interests both from academia and industries. It is a new type of transportation with passengers and cargo traveling in pods at a near-sonic speed through a near-vacuum tube by using the maglev

technology, which can alleviate the mechanical and aerodynamic friction as well as the noise greatly [4]. Since first put forward by Robert Goddard in the 1900s, carried forward by Elon Musk in 2013, and realized by a company named Hyperloop One in 2017, Hyperloop is evolving from the prototype to commercial products exponentially nowadays with worldwide efforts. In 2017, the U.S. company Hyperloop One made history on the world's first hyperloop test track, which achieved historic speeds of 387 km/h on a test track of 500 meters. Furthermore, Hyperloop One accomplished the first passengers' safe-travel on a hyperloop in 2020, making transportation history as reported in the website (https://virginhyperloop.com/). In China, a series of research has been carried out on this new transportation way and some landmarks have been completed. In 2014, Southwest Jiaotong University developed a vacuum pipeline maglev vehicle test system, which is the world's first complete vacuum tube test line with a low air pressure close to the vacuum (0.012 standard atmospheric pressure) and magnetic levitation system.

To guarantee the safe operation of Hyperloops as well as to offer Internet connectivity to the onboard passengers, it is extremely crucial to establish a reliable train-to-ground wireless communication link, which is still at its infant stage [5]. The dedicated communication systems for HSRs have evolved from the global system for mobile communications-railway (GSM-R) to the long-term evolution for railway (LTE-R), which enables high-rate wireless voice and data communications [6]. Meanwhile, the fifth-generation mobile communication system for railway (5G-R) is widely envisioned to shape the future of the railways by offering ultralow latency and ultrahigh reliability based on some technologies like massive multiple-input multiple-output (MIMO), numerology, network slicing, etc. For Hyperloops, the safety-related uRLLC services involve traction control-related services, speed control-related services, sensor monitoring data, emergency messages, etc. Whereas the enhanced mobile broadband (eMBB) services mainly refer to onboard passengers' communications, like online conferences, games, videos, and emails. The former generates low data rates, but poses stringent bit error rate (BER) and latency demands, whereas the latter usually generates chunks of files, but is much more tolerant for BER and latency demands.

The numerology technology of 5G enables a flexible configuration of the physical frame with multiple types of subcarrier spacings and time durations [7]. On this basis, the uRLLC traffic is usually assigned physical resource blocks (PRBs) with short time durations but large bandwidth. In terms of scheduling PRBs, the uRLLC traffic punctures those eMBB users' PRBs in the next mini-slot to satisfy the stringent latency requirements. Currently, extensive works have been conducted in this field, typical works like [8–14]. In [10], Yin et al. proposed a new downlink scheduler for uRLLC multiplexing and aimed to maximize eMBB utility while guaranteeing uRLLC constraints. The resource allocation is formulated as an integer programming (IP) problem and a two-phase solution is presented. In [8], Darabi and Lampe considered different types of uRLLC users with various latency requirements and prioritized uRLLC users with looser latency needs, which is similar to the proposed latency-relaxed concept in this paper. In [11], Alsenwi et al. presented a risk-sensitive based formulation to allocate PRB resources to uRLLC traffic, which aims to minimize the risk of the eMBB transmission and ensure the uRLLC reliability. The drawback of this method is the time-consuming iteration when searching for the solution. In [12], Esswie and Pedersen proposed an enhanced spatial preemptive scheduler for the joint transmission of uRLLC and eMBB traffics, and it aims to provide the sporadic uRLLC traffic with an interference-free subspace for immediate and secured transmission without queuing. In [13], Alsenwi et al. formulated an optimization problem aiming to maximize the eMBB throughput while subject to a uRLLC reliability constraint. A deep reinforcement learning (DRL) based framework is also proposed to solve this problem. In [14], the authors formulated an optimization problem aiming to maximize the minimum expected achieved rate (MEAR) of eMBB users while guaranteeing the requirements of the uRLLC traffic. The decomposition trick is used to divide it into two subproblems.

The aforementioned works investigate the multiplexing problem of uRLLC and eMBB traffic mainly from the aspects of eMBB throughput and uRLLC reliability and propose some corresponding effective solutions. Nonetheless, most of them treat all kinds of uRLLC traffics as a whole and ignore their diverse demands, failing to provide the dedicated services for uRLLC users consequently. As such, we proposed a service-aware concept of multiplexing and used the greedy strategy to solve the issue in [15]. However, this work only focuses on the optimization of uRLLC power, and the eMBB performance remains to be investigated. Besides, the greedy strategy is used to solve the problem, which can handly obtain the optimal/suboptimal solution.

In summary, our main contributions are presented as follows:

(1) Regarding the safety-related Hyperloop train-to-ground communication services, 6 types of uRLLC traffic are assigned with 5 levels according to different latency and BER metrics. Besides, the latency constraint for each type is relaxed properly, which means that the corresponding multiplexing task should be finished no longer than the relaxed latency

(2) We formulate an optimization problem that considers both minimizing the uRLLC energy cost and maximizing eMBB throughput. The relaxed latency-frequency limitation range and BER requirement are considered as 3 key constraints for this problem

(3) To solve this nondeterministic polynomial- (NP-) hard problem, we utilize the particle swarm optimization (PSO) algorithm. Specifically, the unsolved multiplexing positions for uRLLC traffic are regarded as a particle, and the velocity and position information of particles are updated by iteration. The corresponding simulation results are presented

The remainder of this paper proceeds as follows. In Section 2, uRLLC services for Hyperloops are analyzed in detail

with the PRB mapping relationship. Section 3 presents the proposed system model, and we formulate it into a multiobjective optimization problem. Then, the PSO algorithm is introduced to solve this problem in Section 4. Simulation results and analyses are given in Section 5. Finally, conclusions are drawn in Section 6.

2. URLLC Services for Hyperloop

A 5G-based train-to-ground wireless communication architecure for Hyperloop is presented in Figure 1. A two-hop relay strategy is also used to overcome the pod-body penetration attenuation, where the leaky-wave emits and receives signals via wire cables to the track-side active antenna units (AAUs). The pod travels inside the vacuum metal tube at an ultrahigh velocity with an antenna embedded on the top to assemble all onboard communication services. Related works have proven that the leaky waveguide system can provide a steady received signal under this circumstance. Detailed depicts can be found in our previous work [3, 16].

2.1. Customized PRB Mapping for uRLLC. According to some research like [4], the communication services for Hyperloop have some similarities to the LTE-R and 5G-R. In [3, 16], we have already presented detailed analysis on communication services with accurate key performance indicators (KPIs) from the aspects of service type, data rate, end-to-end latency, and bit error rate (BER), which is presented in Table 1.

From a safety-related perspective, the train-to-ground communication services can be classified into 2 types, i.e., uRLLC and eMBB services. Generally speaking, uRLLC services for Hyperloop involve the traction control system (TCS), operation control system (OCS), operational voice communication system (OVCS), train operation status monitoring (TOSM), video surveillance (VS), and passenger information service (PIS). As seen in Table 1, each type of uRLLC service owns a distinct metric when operating. As such, we classify these services into 5 types according to different latency, and BER demands presented in the last column in Table 1. Moreover, we assign PRBs with different time-frequency sizes to each uRLLC traffic by adopting the 5G numerology. As illustrated in Figure 2, we assign PRBs with short time duration and large frequency bandwidth to those high-level uRLLC traffic, which are strict with transmission latency and BER. Whereas low-level uRLLC traffic is allocated with PRBs of long time duration and narrow bandwidth. This special design enables a flexible PRB schedule policy, i.e., the core concept of numerology technology.

As for the eMBB traffic, they are scheduled at the unit of slot and subcarrier. Since we mainly focus on the multiplexing uRLLC traffic of different levels, we present a brief analysis of the fairness among the eMBB users. The proportional fair (PF) algorithm is used to schedule the PRB resources for this systems with multiple carriers. This algorithm aims to maximize the sum of logarithmic average user rates [17]. Specifically, user i is assigned a priority p_i for scheduling at time t, which can be calculated as

$$p_i = \frac{r_i(t)}{R_i(t)}, \tag{1}$$

where $r_i(t)$ is the instantaneous transmittable rate at the current slot, and $R_i(t)$ means the average date rate until the previous slot.

2.2. Latency Relaxation Strategy. In terms of the coexistence of both uRLLC and eMBB traffic, the already allocated PRBs for eMBB are usually punctured by uRLLC traffic to guarantee its transmission priority, i.e., the core concept of multiplexing scheme. Usually, the conventional multiplexing concept means that the arrived uRLLC traffic is arranged to puncture eMBB PRBs at the next mini-slot regardless of the service type. Herein, we propose a latency relaxation scheme, i.e., relax the latency constraint for each type of uRLLC service properly.

Figure 3 presents a diagram of our proposed latency-relaxed uRLLC multiplexing scheme. We can learn from this figure that 4 kinds of uRLLC traffic arrive sporadically and they are assigned with PRBs of different sizes. The higher level is, the shorter time duration of the PRB is. All uRLLC PRBs are superimposed on 4 eMBB users' PRBs directly, which are identified by different colors. Furthermore, the uRLLC traffic of different levels is expected to be multiplexed within a relaxed latency margin. Obviously, high-level uRLLC traffic owns a shorter relaxed margin. For example, a level-3 uRLLC traffic arrives at the 3rd mini-slot and it should be handled within 4 mini-slots. Whereas a level-5 uRLLC traffic arrives at the 2nd mini-slot and is processed at the next mini-slot.

3. System Model

To start with, some important variable notations should be clarified. A physical frame is assumed to cover a time duration of T_0 and a bandwidth of B_0. Besides, it can be divided by N_t mini-slots in the time domain and N_f subcarriers in the frequency domain, which infers that the PRB scheduling unit is $\Delta t \times \Delta f$, where $\Delta t = T_0/N_t$ is the time duration of a mini-slot, and $\Delta f = B_0/N_f$ is the bandwidth of a subcarrier. (t, f) denotes the t-th mini-slot and the f-th subcarrier of a mini-resource element (RE). Note that a mini-RE is regarded as the resource scheduling unit for the uRLLC traffic in this paper. On this basis, the channel gain over the (t, f)-th mini-RE is denoted as $h_{t,f}$. Some important variables and the corresponding definitions are listed in Table 2.

If no uRLLC traffic exists, the allocated uRLLC power at (t, f) is $p_{t,f}^{\mathrm{uRL}} = 0$, and the optimization goal is to maximize the eMBB throughput. We assume that two different power controllers are used for eMBB and uRLLC services, and the eMBB controller operates at a constant power of P_0. Under this case, the water-filling algorithm can be used to obtain the maximum eMBB throughput [18], and the power

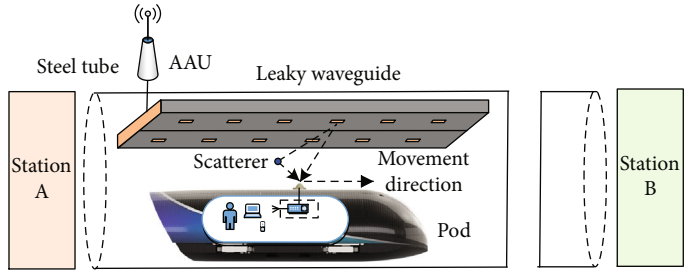

Figure 1: Schematic of the train-to-ground communication system for Hyperloop.

Table 1: Demand analysis of train-ground communication service for the Hyperloop.

Services	Data rate	Latency	BER	Level
uRLLC				
TCS	200 kbps	1 ms	10^{-6}	5
OCS	400 kbps	40 ms	10^{-6}	4
OVCS	32 kbps/channel	40 ms	10^{-5}	3
TOSMS	1 Mbps	50 ms	10^{-5}	3
VSS	18 Mbps	300 ms	10^{-3}	2
PIS	8 Mbps	300 ms	10^{-3}	1
eMBB				
Multimedia	0.4-4 Gbps	—	—	0

TCS: traction control service; OCS: operation control service; OVCS: operational voice communication service; TOSMS: train operation status monitoring service; VSS: video surveillance service; PIS: passenger information service.

allocated to N_f subcarriers at a specific time can be calculated as

$$p_{t,f}^{\mathrm{eMB}} = \max\left(\mu - n_0 \Delta f / \left|h_{t,f}\right|^2, 0\right), \tag{2}$$

$$\sum_{f=1}^{N_f} p_{t,f}^{\mathrm{eMB}} = P_0, \tag{3}$$

where $p_{t,f}^{\mathrm{eMB}}$ is the eMBB power at (t,f) to be solved, n_0 denotes the noise power spectral density (nPSD), and μ is an auxiliary solution variable. Then, the maximum capacity over (t,f) can be calculated as

$$C_{t,f}^{\mathrm{eMB}} = \Delta f \log_2\left(1 + \frac{p_{t,f}^{\mathrm{eMB}} h_{t,f}}{n_0 \Delta f}\right). \tag{4}$$

As for the coexistence case of uRLLC and eMBB services, the multiplexing scheme is used, and it implies that uRLLC PRBs puncture eMBB PRBs by preemption. Suppose a bunch of uRLLC traffic with a number of Q^{uRL} arrives sporadically at the t_{arr}-th mini-slot. Assume the level of the q-th traffic is $s \le S$ $(s \in \mathbb{N}^*)$, where S means the maximal uRLLC level number. The corresponding multiplexing relaxation latency is denoted as $d_s \Delta t, (d_s \in \mathbb{N}^*)$, and the required BER is marked as P_s^{req}. The PRB size is expressed as $N_T^s \times N_B^s, (N_T^s, N_B^s \in \mathbb{N}^*)$ mini-REs, which can be regarded as a rectangle with a start position (SP) marked as (t_{q0}^s, f_{q0}^s). As such, the preempted PRB area of the q-th uRLLC traffic can be expressed as

$$\Omega_q^s = \left[t_{q0}^s, t_{q0}^s + N_T^s - 1\right] \times \left[f_{q0}^s, f_{q0}^s + N_B^s - 1\right]. \tag{5}$$

For an uRLLC traffic of the s-th level, its corresponding PRB size can be expressed $2^{S-s}\Delta t \times 2^s \Delta f$ considering the numerology technology. Considering the time-frequency constraints, i.e., the relaxed latency margin and subcarrier number, the SP of the q-th uRLLC traffic is given as

$$1 \le t_{q0}^s - t_{arr} \le d_s, t_{q0}^s \in \mathbb{N}^*, \tag{6}$$

$$1 \le f_{q0}^s \le N_f - N_B^s, f_{q0}^s \in \mathbb{N}^*, \tag{7}$$

where (6) means that for a given q-th uRLLC traffic with a level of s, the maximum delay range should be considered when multiplexing. In other words, the multiplexing delay margin is constrained by the corresponding predetermined delay setting d_s. The meaning of (7) is much similar to (6). It reveals that the multiplexing frequency range should not exceed the maximal frequency range. Considering its PRB size, the maximal frequency range is set to $N_f - N_B^s$.

Another necessary constraint is the uRLLC BER requirements, which are strictly related to the wireless channel status. Assume the M-quadrature amplitude modulation (QAM) modulation is adopted for all uRLLC traffic, and the corresponding BER over additive white Gaussian noise (AWGN) channel is expressed as [19].

$$P_e = \frac{\sqrt{M} - 1}{\sqrt{M}\log_2\sqrt{M}} \operatorname{erfc}\left(\sqrt{\frac{3\log_2 M}{2(M-1)}\widehat{\gamma}}\right), \tag{8}$$

where $\widehat{\gamma}$ is the estimated signal to interference plus noise ratio (SINR). Obviously, BER is determined by the parameter M and $\widehat{\gamma}$. When multiplexing, the BER of the q-th uRLLC traffic should satisfy

$$P_q^s\left(M, \widehat{\gamma}_q^s\right) \le P_s^{\mathrm{req}}. \tag{9}$$

This constraint involves the BER requirement. Specifically, the BER of an uRLLC traffic after multiplexing should

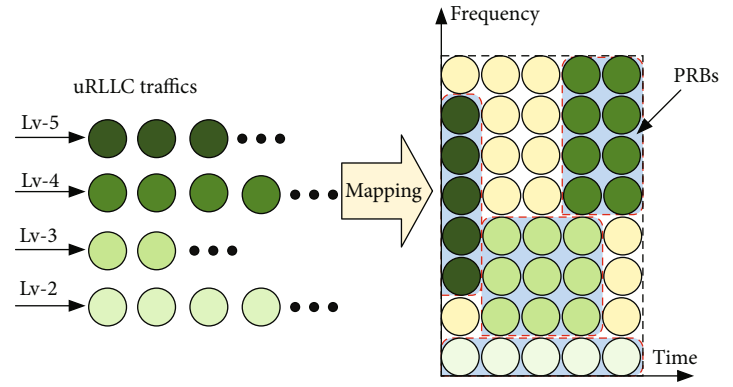

Figure 2: Schematic of the mapping uRLLC to different PRBs.

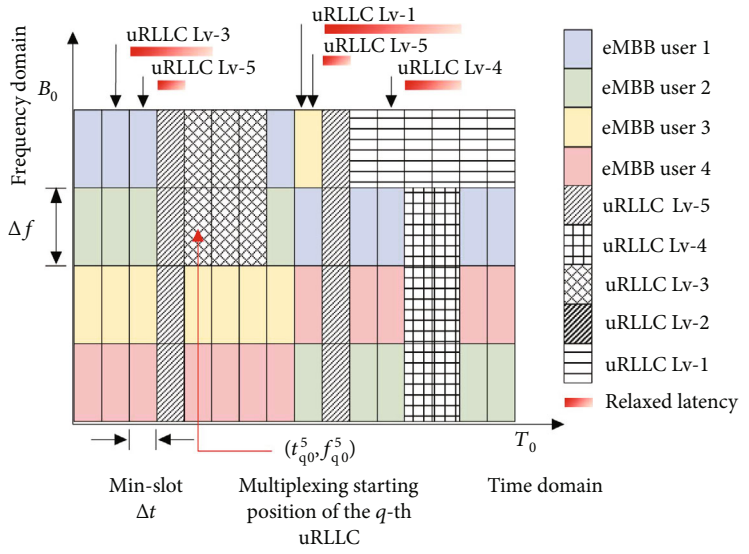

Figure 3: A diagram of the proposed latency-relaxation based multiplexing.

Table 2: Summary of key parameter definitions.

Variable	Definition	Variable	Definition
B_0	System bandwidth	n_0	nPSD
N_t, N_f	Number of mini-slots and subcarriers within a frame	$\Delta t, \Delta f$	Mini-slot duration time and subcarrier bandwidth
(t, f)	Index of the RE	$h(t, f)$	Channel gain at the (t, f)-th RE
$p^{\text{eMB}}_{t,f}$	eMBB power over the (t, f)-th RE	$p^{\text{uRL}}_{t,f}$	uRLLC power over the (t, f)-th RE
d_s	Maximum latency of level s	P^{req}_s	Required BER of level s
N^s_T, N^s_B	PRB time and frequency size level s	t^s_{q0}, f^s_{q0}	PRB start position of the q-th uRLLC traffic with a level of s
$\widehat{\gamma}^s_q$	SINR of the q-th URLLC traffic	$p^s_{q,O}$	PRB position center of the q-th traffic

satisfy its predetermined requirement to guarantee high transmission reliability. For the M-QAM, the corresponding $\widehat{\gamma}^s_q$ for the q-th uRLLC traffic can be expressed as

$$\widehat{\gamma}^s_q = \frac{\sum_{(t_q,f_q)\in\Omega^s_q} p^s_{t_q,f_q} \left\| h_{t_q,f_q} \right\|^2}{\sum_{(t_q,f_q)\in\Omega^s_q} p^{\text{eMB}}_{t_q,f_q} \left\| h_{t_q,f_q} \right\|^2 + N_{s,0}}, \tag{10}$$

where $N_{s,0} = n_0 N^s_T N^s_B \Delta f$ is the noise power over PRB Ω^s_q. $p^s_{t_q,f_q}$ and $p^{\text{eMB}}_{t_q,f_q}$ denote the allocated power of the q-th uRLLC traffic and eMBB traffic at the PRB position (t_q, f_q), respectively. It is noteworthy that the variable $\widehat{\gamma}^s_q$ is calculated for the uRLLC traffic. When calculating the eMBB capacity/throughput, similar derivations can be formulated where uRLLC power is regarded as interference.

Table 3: Validation layout parameters.

Parameters	Settings
Population size	100
Iteration	500
Safety level	[1–5]
RB size	$[16, 8, 4, 2, 1]\Delta t \times [1, 2, 4, 8, 16]\Delta f$
Relaxed latency	[30,20,15,10,5] Δt
BER metrics	$[10^{-3}, 10^{-4}, 10^{-5}, 10^{-6}, 10^{-6}]$
Modulation	16QAM
eMBB power	W
nPSD	-174 dBm/Hz
Carrier frequency	3.55GHz

Without any doubt, the fact that uRLLC traffic preempts those eMBB users' PRBs will inevitably affect the corresponding network throughput. In addition, uRLLC traffic poses strict BER requirements even if being allocated to those PRBs of good channel quality. Therefore, two independent power controllers are used for eMBB and uRLLC separately. Besides, the uRLLC latency and BER requirements should also be guaranteed. Finally, we formulate a dual-objective optimization goal incorporating the minimization of uRLLC power consumption and maximization of eMBB throughputs, which is expressed as

$$2 \min_{\gamma_q^s, p_{t_q,f_q}^s} \max \left\{ \alpha T^{\mathrm{eMB}} - \beta P^{\mathrm{uRL}} \right\}, \tag{11}$$

$$\text{s.t.} \alpha + \beta = 1, \alpha, \beta \in (0, 1), \tag{12}$$

$$T^{\mathrm{eMB}} = \sum_{(t_q,f_q) \notin \Omega_q^s} C_{t,f}^{\mathrm{eMB}} \Delta t, , \tag{13}$$

$$p_q^s = \sum_{(t_q,f_q) \in \Omega_q^s} p_{t_q,f_q}^s, \tag{14}$$

$$\Omega_q^s \cap \Omega_{q'}^{s'} = \varnothing, \tag{15}$$

$$q \neq q', q, q' \in \left\{1, 2, \cdots, Q^{\mathrm{uRL}}\right\}, , \tag{16}$$

where α and β are two parameters used to tune the weights of throughput and power consumption with a constraint of (12). Note that constraints (6), (7), and (9) should also be satisfied. Regarding constraint (15), we neglect those preempted PRBs when calculating eMBB throughput since that uRLLC traffic requires high SINR values to satisfy the strict BER demands, which corrupts those eMBB PRBs severely. p_q^s in (14) represents the total power allocated to the q-th uRLLC traffic. Constraint (15) implies that multiplexing PRB areas of any two uRLLC traffic should not overlap with each other. To this end, the multiplexing coordinate Ω_q^s of each uRLLC traffic and the corresponding allocated power p_{t_q,f_q}^s, $(t_q, f_q) \in \Omega_q^s$ over each mini-RE remain to be solved.

4. Solution Based on PSO

4.1. Reduction of Variables. It is hard to find the optimal/suboptimal solution for (11), especially involving multiple variables. To alleviate the analysis complexity, we first neglect the calculation of the total power of the q-th uRLLC traffic, i.e., p_q^s and assume its value is known in advance. Note that the value of p_q^s will be given later. As for the eMBB power $p_{t,f}^{\mathrm{eMB}}$ allocated at position (t, f), it can be obtained based on (2) and (3). Then, we focus on the uRLLC services and aim to maximize the SINR of the q-th uRLLC traffic γ_q^s with a goal of

$$\max_{p_{t_q,f_q}^s} \left\{ \gamma_q^s \right\}, \tag{17}$$

$$\sum_{(t_q,f_q) \in \Omega_q^s} p_{t_q,f_q}^s = p_q^s. \tag{18}$$

This is a convex problem, which can be solved easily by the Lagrange multiplier method. The corresponding solution can be expressed as

$$p_{t_q,f_q}^s = \frac{\left\| h_{t_q,f_q} \right\|^2 p_q^s}{\sum_{(t,f) \in \Omega_q^s} \left\| h_{t_q,f_q} \right\|^2}. \tag{19}$$

On this basis, we reduce those variables to be solved p_{t_q,f_q}^s, (t_q, f_q) over PRB Ω_q^s to one, i.e., p^s. Until now, 3 variables still need to be solved, i.e., SP (t_{q0}^s, f_{q0}^s) and p^s. Since the eMBB power allocation and noise PSD are already given, then p^s can be obtained by some manipulations of (10), which is

$$p_q^s = \widehat{\gamma}_q^s \frac{\left(\sum_{(t,f) \in \Omega_q^s} p_{t_q,f_q}^{\mathrm{eMB}} \left\| \widehat{h}_{t_q,f_q} \right\|^2 + N_{s,0} \right)}{\sum_{(t,f) \in \Omega_q^s} \left\| \widehat{h}_{t_q,f_q} \right\|^4} \times \left(\sum_{(t,f) \in \Omega_q^s} \left\| \widehat{h}_{t_q,f_q} \right\|^2 \right). \tag{20}$$

From the above formula, we can learn that once the SP (t_{q0}^s, f_{q0}^s) is determined, and the corresponding p_q^s can be calculated to guarantee its BER requirement.

It is a two-dimensional bin packing issue belonging to the NP-hard problem, which is hard or even impossible to search for the optimal solution within a finite time. To this end, some heuristic algorithms like the genetic algorithm (GA), PSO algorithm, and artificial neural network (ANN) are usually adopted to search for the optimal/suboptimal solution through extensive computational iterations. However, this kind of algorithm is time-consuming and sometimes is hard to satisfy the stringent uRLLC latency demands. As such, we can set the maximum iteration time properly according to the specific scenario to obtain the suboptimal or even nonsuboptimal solutions to cater to its latency demands. Herein, we use the widely used PSO

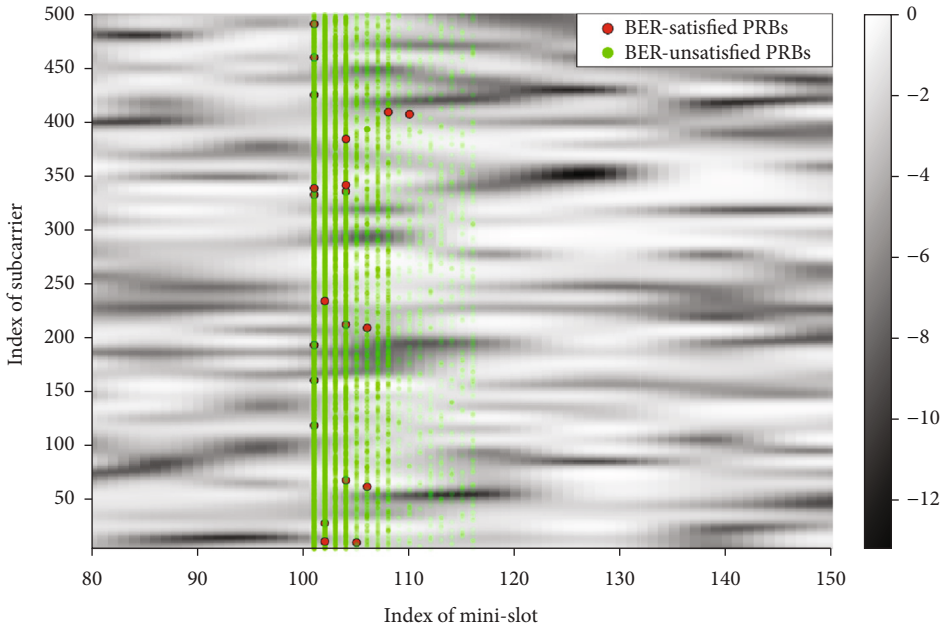

Figure 4: Schematic of the BER results after PSO initialization.

algorithm with the merits of high efficiency and simple implementation, which is inspired by swarm behavior such as bird flocking and schooling in nature.

4.2. PSO-Based Solution. When implementing the PSO, we first generate M_{P} particles. For the m-th particle $\vec{K}_m$, it is made up of a matrix with a dimension of $2 \times Q^{\mathrm{uRL}}$, where the q-th column vector is expressed as $\vec{K}_{q,m} = [p_q^s, t_{q0}^s]^{\mathrm{T}}$. The fitness value of $\vec{K}_m$ is calculated by (11). Our proposed PSO-based solution mainly involves the following steps.

(1) Determine the particle swarm number M_{P}, the maximum iteration epoch N^{iter}, channel gain $h_{t,f}$, the corresponding relaxation latency, and BER requirements for all types of uRLLC traffic

(2) Pack the unsolved positions into a particle and initialize its velocity and position. Calculate the corresponding fitness at the initial position, then take it as the personal best position $\vec{K}_m^{\mathrm{pbest}}$. On this basis, find the global best optimal particle $\vec{K}^{\mathrm{gbest}}$, which can be expressed as

$$\vec{K}^{\mathrm{gbest}} = \arg \min_m \left\{ F\left(\vec{K}_m^{\mathrm{pbest}}\right) \right\}. \tag{21}$$

(3) Update the velocity and position of the m-th particle based on $\vec{K}_m^{\mathrm{pbest}}$ and $\vec{K}^{\mathrm{gbest}}$, i.e.,

$$\vec{V}_m(r+1) = \omega \vec{V}_m(r) + c_1 R_1 \left(\vec{K}^{\mathrm{pbest}} - \vec{K}_m\right) + c_2 R_2 \left(\vec{K}^{\mathrm{gbest}} - \vec{K}_m\right), \tag{22}$$

$$\vec{K}_m = \vec{K}_m + \vec{V}_m(r+1), \tag{23}$$

where $R_1, R_2 \in (0, 1)$ are two random numbers, and $\omega \in (0, 1)$ is a weight to promote local exploitation. c_1, c_2 mean two learning factors. Since that multiplexing position is scheduled at the units of mini-slot and subcarrier, the 2nd and 3rd dimensions for all column vectors of the updated $\vec{K}_m$ are conducted by the rounding operation.

(4) Then, check whether there is any PRBs overlap between any two uRLLC traffic, i.e., the corresponding column vectors. If so, choose a uRLLC traffic randomly and move its PRB to make room for the other one to avoid the multiplexing PRBs coincidence. Specifically, we deal with the uRLLC traffic within a particle in turns. As for the first uRLLC traffic, its position keeps unchanged. Assume the first $(q-1)$ traffic has been handled; then, we focus on multiplexing the next q-th traffic with a level of s. We calculate the distance between its center to the center of the q' traffic. If

$$\left\| p_{q,O}^s - p_{q',O}^{s'} \right\| < \sqrt{\left(0.5N_B^s + 0.5N_B^{s'}\right)^2 + \left(0.5N_T^s + 0.5N_T^{s'}\right)^2}, \tag{24}$$

where $1 \le q' \le q-1$, i.e., these two PRBs overlap with each other. If they overlap in the delay domain; then, the

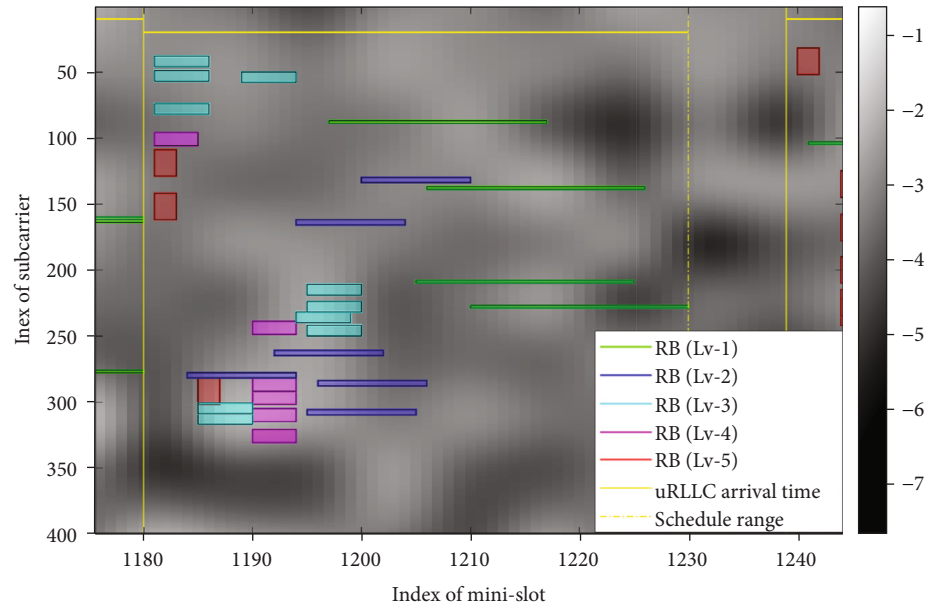

(a)

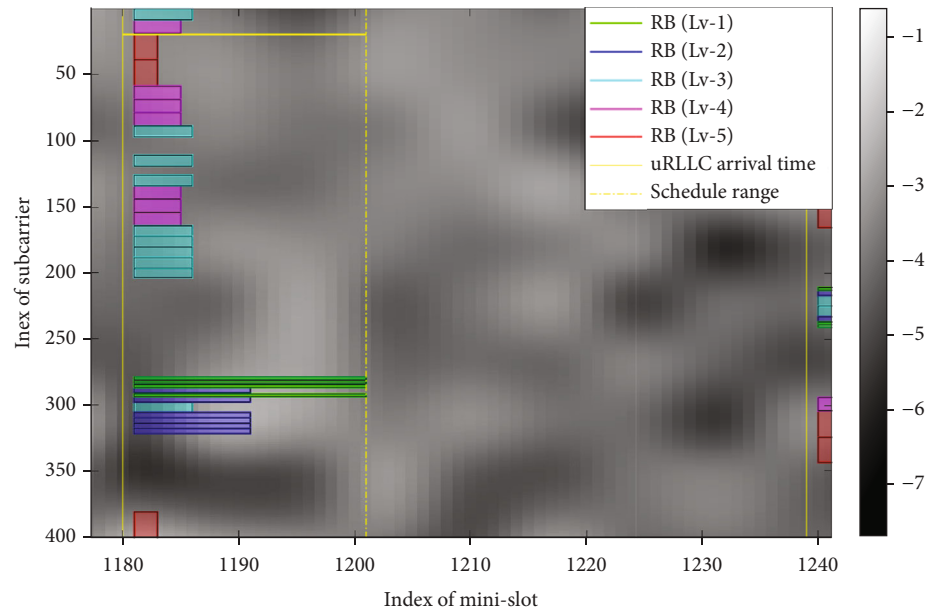

(b)

Figure 5: Schematic of the BER results after PSO initialization when $\alpha = \beta = 0.5$, (a) relaxed latency margin, and (b) no latency margin.

position of q' traffic is changed to

$$t_{q0}^{s} = t_{q'0}^{s'} + \mathrm{sgn}\left(t_{q0}^{s} - t_{q'0}^{s'}\right) \times \left(0.5N_T^{s} + 0.5N_T^{s'} - \left\|t_{q0}^{s} - t_{q'0}^{s'}\right\|\right). \tag{25}$$

Likewise, if they overlap in the frequency domain, the same operation is performed. Note that the updated position should not exceed both the delay and frequency boundaries.

(5) Check the constraints of all particles and calculate the fitness after updating. If any of the constraints is not satisfied, an additional penalty is added to the fitness value. Update $\vec{K}^{\mathrm{pbest}}$ and $\vec{K}^{\mathrm{gbest}}$ based on (23).

(6) Check if the iteration termination condition is met. If so, return $\vec{K}^{\mathrm{zbest}}$ and terminate the flow. Otherwise, go to Step 3

5. Simulation Analysis

In the simulation, the scheduling unit for uRLLC traffics takes up the duration of a mini-slot of 0.1 ms and a subcarrier of 180 kHz, whereas that for eMBB is set to a slot and a

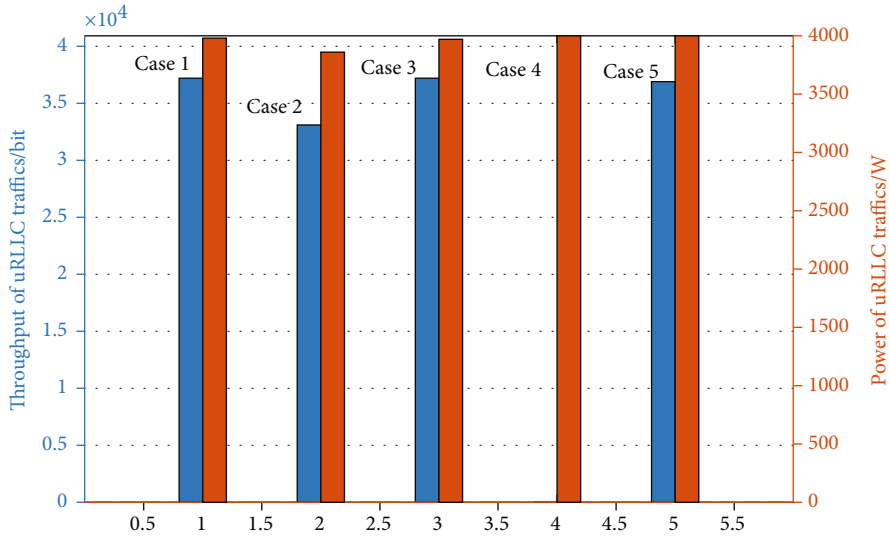

Figure 6: Power consumption and eMBB throughput of different schemes.

Table 4: Results comparison of 4 cases.

Parameters (α, β)	uRLLC power/kW	eMBB throughput/kbit
(0, 1)	3.98	37.2
(1, 0)	3.86	33.1
(0.5,0.5)	3.97	37.2
[15]	4.0	—
No margin	4.0	36.9

Table 5: Comparisons of computational time.

Scheme	Computational time/sec
PSO-based scheme	420.5
Conventional scheme	0.55
Greedy strategy in [15]	8.6

subcarrier based on the 5G settings. Assume $N_f = 400$ subcarriers are used and nPSD $n_0 = -174$ dBm/Hz, and all uRLLC traffic adopts the 16QAM modulation regardless levels. Taking the various uRLLC latency and BER requirements into account, we classify these services into 5 different levels with specific demands according to [16], and the corresponding parameters and values are listed in Table 1. To start with, the predominant task is to find an accurate channel model to characterize the propagation scenario. We adopt the leaky waveguide system to realize the pod-to-ground communication as presented in Figure 1. As reported in [3], the propagation model can be approximated as the Rician channel by designing a special leaky-wave system that can depress the Doppler effect. The received power decays as the transceiver distance increases along the central axis of the pipeline. As such, the corresponding channel can be expressed as

$$h = \sqrt{\frac{P_0 e^{-\gamma r}}{d_{TR}^2}} \cdot \mathscr{R}, \tag{26}$$

where P_0 is the transmit power, which is set to 1 W. d_{TR} means the separation distance between transmitter (Tx) and receiver (Rx) in the tube cross-section with a value of 0.5 m. r is the horizontal Tx-Rx separation distance, with a maximal distance of 50 m. Parameter γ denotes the decay factor, and it is set to 0.03 herein. $\mathscr{R}$ represents the Rician channel with a K-factor of 13 dB according to the simulation results in [20]. Other detailed simulation results are presented in Table 3.

In [16], the authors take the multiplexing positions and power as a particle, and the initially generated particles with different positions are plotted in Figure 4. A bunch of particles with random positions and velocities is obtained, where the green dots in the figure indicate uRLLC traffic that fails to meet the BER requirements after checking all constraints, whereas those red dots mean the legal particles that satisfy all constraints. It can be seen that most of the initial particles fail to satisfy the BER requirement if neglected (20). As such, (20) can not only be used to reduce the variable number but also calculate the required power for a given multiplexing position. Further optimization procedures are conducted based on this formula.

Figure 5 demonstrates a schematic diagram of our proposed latency-relaxation multiplexing scheme when $\alpha = 0.5$ and $\beta = 0.5$, where subfigure (a) denotes the proposed scheme with a relaxed latency margin, and subfigure (b) means the conventional scheme which adopts no latency margin. As shown in this figure, 29 uRLLC services with 5 different levels, i.e., different PRB sizes arrive at the 1180th mini-slot. After 500 times of iterations, the multiplexing positions of RBs with different levels are obtained based on the proposed PSO algorithm, and they are plotted as rectangles with different sizes. The background color represents the normalized channel gain in the unit of a decibel at the

corresponding PRB location, where the solid yellow line on the left vertical axis means the arrival time of uRLLC traffic, and the dotted yellow line on the right vertical axis refers to the relaxation latency including the time duration of resource blocks. Obviously, different tunes of α and β result in totally different allocation results.

Since the eMBB throughput deteriorates as uRLLC traffic preempts its PRBs, we focus on the eMBB throughput of preempted PRBs and aim to maximize it regardless of other unoccupied PRBs. Figure 6 compares the throughput and power results of uRLLC traffic for different α and β values. 3 cases are considered as follows.

(1) *Case 1*. $\alpha = 0, \beta = 1$. This policy tries to maximize the eMBB throughput regardless of the uRLLC power consumption. Consequently, the obtained multiplexing positions usually involve those PRBs of poor channel quality, like the green PRB in Figure 5

(2) *Case 2*. $\alpha = 1, \beta = 0$. In this case, the optimization problem aims to minimize the consumption power of the uRLLC traffic and neglect the eMBB throughput. The results indicate that it consumes the minimum power of all cases. However, this satisfying effect is achieved at the expense of throughput

(3) *Case 3*. $\alpha = 0.5, \beta = 0.5$. This case considers both eMBB throughput and uRLLC power consumption. The results reveal that this configuration presents a good tradeoff between the eMBB throughput and uRLLC power consumption, proving to be a better option

(4) *Case 4*. The greedy multiplexing strategy in [15]. Since that [15] focuses on the uRLLC consumption, we tune $\alpha = 1$ and $\beta = 0$ in this case. As such, the throughput result is 0. The greedy strategy is used to obtain the solution, and the results indicate that it costs the highest uRLLC power of all cases, which means that the PSO can acquire a better multiplexing solution

(5) *Case 5*. The conventional multiplexing scheme. It means that all uRLLC traffic should be processed in the next mini-slot

Finally, we list detailed numerical results in Table 4. Compare our proposal $(\alpha = 0.5, \beta = 0.5)$ with the conventional scheme, i.e., multiplexing in the next mini-slot and the scheme in [15]. It can be seen that the conventional scheme has few multiplexing positions, and our proposed latency-relaxed concept provides better performance. Besides, the PSO-based solution yields a good tradeoff between the uRLLC consumption power and eMBB throughput. Furthermore, we compare the computational complexity of these 3 different schemes. The simulation is conducted on a MATLAB platform and operates on an x64 system with an Intel Core i7 CPU@2.60GHz, which is presented in Table 5. Obviously, our proposal consumes more time to obtain a better multiplexing solution. For further communication application in Hyperloops, the maximal iteration number and particle swarm number can be set appropriately based on the computational capacity of operation systems.

6. Conclusion

In this paper, we propose a novel latency-relaxation concept of multiplexing uRLLC and eMBB traffic for Hyperloop communications by using the flexibility of 5G numerology technology. An optimization problem that aims to minimize the uRLLC power consumption and maximize the eMBB throughput is formulated, and the latency together with BER requirements are considered as constraints. Furthermore, a PSO-based algorithm is used to cope with this NP-hard problem. The simulation results verify the energy-saving and less interference on eMBB throughput compared to the conventional scheme.

Data Availability

The data used to support the findings of this study are available from the corresponding author upon request.

Conflicts of Interest

The authors declare that there is no conflicts of interests regarding the publication of this paper.

Acknowledgments

This research was supported in part by the Beijing Natural Science Foundation under grant L201012, the Fundamental Research Funds for the Central Universities under grant 2018JBZ102, and the National Natural Science Foundation of China under grant 62001139.

References

[1] K. Guan, B. Ai, B. L. Peng et al., "Towards realistic high-speed train channels at 5G millimeter-wave band—part I: paradigm, significance analysis, and scenario reconstruction," *IEEE Transactions on Vehicular Technology*, vol. 67, no. 10, pp. 9112–9128, 2018.

[2] X. Press, *China's High-Speed Rail Lines Top 37,900 Km at End of 2020*Jan. 2021, http://www.china.org.cn/business/2021-01/10/content_77099157.htm.

[3] C. Qiu, L. Liu, B. Han, J. Zhang, Z. Li, and T. Zhou, "Broadband wireless communication systems for vacuum tube high-speed flying train," *Applied Sciences*, vol. 10, no. 4, p. 1379, 2020.

[4] W. Hedhly, O. Amin, B. Shihada, and M.-S. Alouini, "Hyperloop communications: challenges, advances, and approaches," *IEEE Open Journal of the Communications Society*, vol. 2, pp. 2413–2435, 2021.

[5] A. Tavsanoglu, C. Briso, D. Carmena-Cabanillas, and R. B. Arancibia, "Concepts of hyperloop wireless communication at 1200 km/h: 5G, Wi-Fi, propagation, Doppler and handover," *Energies*, vol. 14, no. 34, pp. 983–996, 2021.

[6] R. He, B. Ai, G. Wang et al., "High-speed railway communications: from GSM-R to LTE-R," *IEEE Vehicular Technology Magazine*, vol. 11, no. 3, pp. 49–58, 2016.

[7] S.-Y. Lien, S.-L. Shieh, Y. Huang, B. Su, Y. L. Hsu, and H. Y. Wei, "5G new radio: waveform, frame structure, multiple access, and initial access," *IEEE Communications Magazine*, vol. 55, no. 6, pp. 64–71, 2017.

[8] M. Darabi and L. Lampe, *Multi Objective Resource Allocation for Joint eMBB and URLLC Traffic with Different QoS Requirements*, 2019 IEEE Globecom workshops (GC Wkshps), Waikoloa, HI, USA, 2020.

[9] J. Zhang, X. Xu, K. Zhang, B. Zhang, X. Tao, and P. Zhang, "Machine learning based flexible transmission time interval scheduling for eMBB and uRLLC coexistence scenario," *IEEE Access*, vol. 7, pp. 65811–65820, 2019.

[10] H. Yin, L. Zhang, and S. Roy, "Multiplexing URLLC traffic within eMBB services in 5G NR: fair scheduling," *IEEE Transactions on Communications*, vol. 69, no. 2, pp. 1080–1093, 2021.

[11] M. Alsenwi, N. H. Tran, M. Bennis, A. K. Bairagi, and C. S. Hong, "eMBB-URLLC resource slicing: a risk-sensitive approach," *IEEE Communications Letters*, vol. 23, no. 4, pp. 740–743, 2019.

[12] A. A. Esswie and K. I. Pedersen, *Capacity Optimization of Spatial Preemptive Scheduling for Joint URLLC-eMBB Traffic in 5G New Radio*, 2018 IEEE Globecom Workshops (GC Wkshps), Abu Dhabi, United Arab Emirates, 2018.

[13] M. Alsenwi, N. H. Tran, M. Bennis, S. R. Pandey, A. K. Bairagi, and C. S. Hong, "Intelligent resource slicing for eMBB and URLLC coexistence in 5G and beyond: a deep reinforcement learning based approach," *IEEE Transactions on Wireless Communications*, vol. 20, no. 7, pp. 4585–4600, 2021.

[14] A. K. Bairagi, M. S. Munir, M. Alsenwi, N. H. Tran, S. S. Alshamrani, and M. Masud, "Coexistence mechanism between eMBB and uRLLC in 5G wireless networks," *IEEE Transactions on Communications*, vol. 69, no. 3, pp. 1736–1749, 2021.

[15] J. C. Zhang and L. Li, "A greedy strategy of multiplexing uRLLC traffic within eMBB services for HSR," in *2021 7th International Conference on Computer and Communications (ICCC)*, Chengdu, China, Dec. 2021.

[16] J. Zhang, L. Liu, B. Han et al., "Concepts on train-to-ground wireless communication system for Hyperloop: channel, network architecture, and resource management," *Energies*, vol. 13, no. 17, pp. 4309–4329, 2020.

[17] H. Kim and Y. Han, "A proportional fair scheduling for multicarrier transmission systems," *IEEE Communications Letters*, vol. 9, no. 3, pp. 210–212, 2005.

[18] D. P. Palomar and J. R. Fonollosa, "Practical algorithms for a family of waterfilling solutions," *IEEE Transactions on Signal Processing*, vol. 53, no. 2, pp. 686–695, 2005.

[19] K. Cho and D. Yoon, "On the general BER expression of one- and two-dimensional amplitude modulations," *IEEE Transactions on Communications*, vol. 50, no. 7, pp. 1074–1080, 2002.

[20] B. T. Han, J. C. Zhang, L. Liu, and C. Tao, "Position-based wireless channel characterization for the high-speed vactrains in vacuum tube scenarios using propagation graph modeling theory," *Radio Science*, vol. 55, no. 4, pp. 1–12, 2020.